Design and fabrication of a high-Q near-field probe for subsurface crack detection

E. Nemati mahkouye[1], J. Ahmadi- shokouh[1], F. Kazemi[2]
[1]*Department of Communications Engineering, University of Sistan and Baluchestan, Zahedan, Iran*
[2]*Engineering Department, University of Zabol, Zabol, Iran*
E_n9281@ymail.com, jahmadis@ieee.org, Fkazemi@uoz.ac.ir
Corresponding author:jahmadis@ieee.org

***Abstract*-Non-destructive detection and evaluation of invisible cracks in metal structures is an important matter in several critical environments including ground transportation, air transportation and power plants. In this paper, a high-Q near-field Microwave probe is designed and fabricated using defected ground structures for surface and subsurface crack detection in metal structures. For this purpose, several near-field probes with different DGSs are designed and probe with the highest quality factor is selected for subsurface detection. Experimental results show that the proposed probe is able accurately detect invisible crack of a size 1mm with at least 20dB magnitude and more than 300 degrees phase contrast. It has also been demonstrated that the proposed device can efficiently used for detection and imaging of small failure and crack in dielectric and metallic structures. Also, it is noted that if the probe dimensions scale down, spatial resolution for crack detection of size in micro and nanometer is achieved at millimeter waves.**

***Index Terms*-**Microwave imaging, near-field probe, defected ground structures, crack detection.

I. INTRODUCTION

Microwave imaging techniques cover almost all important applications of electromagnetism, such as remote sensing technology [1, 2], non-destructive testing and evaluation [3], geophysical surveying [4] and medical diagnostics [5-7]. Moreover, a near-field microwave scanning has the unique ability to provide direct images of subsurface structures with nearly atomic resolutions, owing to the penetration and possible resonant absorption of its electromagnetic signal inside materials [8-11]. In many sensing and imaging problems, the object is covered by some medium that conceals or obscures its relevant features. The object may emit some wave and field that penetrate the medium and may be observed by a detector. Alternatively, a wave or a field may be used as a probe that travels through the medium and is modified by the object before it travels back through the medium on its way to the detector. The challenge is to extract information about the subsurface target in the presence of the obscuring medium [12].

Manuscriptreceived17-June-2017 and revised 6-Nov.-2017, P-ISSN:2322-4088
Accepted on 20- Jan.-2018 *E- ISSN: 2322-3936*

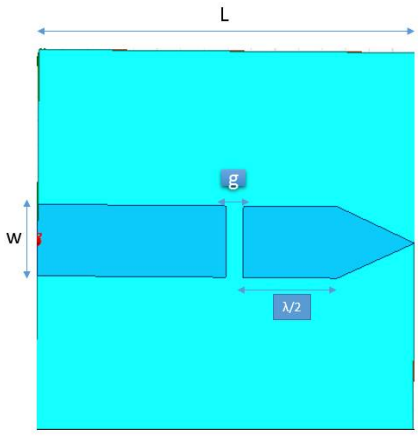

Fig. 1. Schematic of primary probe

Crack or failure in the metallic structure such as aircraft fuselage, nuclear power plant steam generator tubing and steel bridges usually begins from the surface but it may be covered by a layer of paint and cannot be visible [13].Hence, detection of this failure and crack in metallic structures is the most importance to the on-line and in-service inspections of critical metallic components. There are several nondestructive evaluation techniques (NDE) for crack detection in metal components and each method has limitations and disadvantages [14-18]. For example, in some cases such as cracks under paint coatings in aircraft fuselage, some of these techniques are not able to detect failures. Therefore, there is a need for very accurate NDE techniques for surface and subsurface detections. In this paper a high-Q near-field probe based on 2D micro-strip line construction using defected ground structures at 18.5GHz is proposed and experimentally evaluated for subsurface detection of cracks in metal structures. For this purpose, several near-field probes with different DGSs are designed and probe with the highest quality factor is selected for subsurface detection. Then, a measurement scenario for detection of invisible cracks with different sizes is implemented. Experimental results show that the proposed probe is able to detect the crack of size larger than 1mm with at least 20dB magnitude and more than 300 degrees phase contrast. Also, it is noted that if the probe dimensions scale down, spatial resolution for crack detection of size in micro and nanometer is achieved at millimeter waves. There are many reported research on crack detection [3-4] but unique advantage of this study is application of the proposed imaging system in subsurface detection of cracks and failures.

II. DESIGN OF HIGH QUALITY NEAR-FIELD PROBE

A. Primary Probe

Fig. 1 demonstrates the general structure of the near-field probe based on 2D micro-strip line geometry. This structure is designed based on two primary points as follows: (a) return loss must be minimized for incensement of the probe's sensitivity; (b) tip of the probe must be sharpest as much as possible for achieving images with good resolution [19]. In the first case a cavity resonator is used to

Table I. Probe Characteristics (all dimensions in mm)

ε_r	ε_e	tanδ	Z_0	w	L	g
4.4	4.18	0.02	50	3mm	16mm	0.73mm

minimize the return losses and the effect of the gap, which is investigated for the probe performances. In the second case to attain high resolution, the probe with different angles according to their sharpness is studied, and the best tip is also selected.

Operation principles of a 2D micro-strip near-field probe are explained in [19-20]. For a micro-strip resonator constructed from a λ/2 length of 50 open-circuited micro-strip line, a substrate is FR4 (ε_r =4.4, tanδ=0.02) with a thickness of 1.6mm, and the conductors are copper. The effective dielectric constant of a microstrip line is given approximately by equation (1). For given characteristic impedance $Z_O$and dielectric Constant ε_r, the *W/d* ratio can be found as shown in equations (2-3).

$$\varepsilon_e = \frac{\varepsilon_r + 1}{2} + \frac{\varepsilon_r - 1}{2}\frac{1}{\sqrt{1+12d/W}} \tag{1}$$

$$W/d = \begin{cases} \dfrac{8e^A}{e^{2A}-2} & for \quad W/d < 2 \\ \dfrac{2}{\pi}\left[B - 1 - \ln(2B-1) + \dfrac{\varepsilon_r - 1}{2\varepsilon_r}\left\{\ln(B-1) + 0.39 - 0.61/\varepsilon_r\right\}\right] & for \quad W/d > 2 \end{cases} \tag{2}$$

$$A = \frac{Zo}{60}\sqrt{\frac{\varepsilon_r + 1}{2}} + \frac{\varepsilon_r - 1}{\varepsilon_r + 1}(0.23 + 0.11/\varepsilon_r) \tag{3}$$

$$B = \frac{377\pi}{2Zo\sqrt{\varepsilon_r}}$$

The probe structure in Fig. 1 is numerically investigated for several tips with different sharp angle applying the HFSS based on the Finite Element Method (FEM) [21] and the best sharp angle for achieving a minimum return loss is obtained 49 degrees. Also, the effect of the air gap on the probe performances is investigated and the best air gap for the good return loss of the probe is selected 0.73mm. Final computation of all the probe structure dimensions for resonating at 18.5GHz is summarized in Table I and the simulation result for the return loss of the probe is shown in Fig. 2. The quality factor (Q) for the primary probe is obtained 220. In the next section, several structures of DGSs for enhancement of probe's quality factor are implemented on the geometry of primary probe.

B. Enhancement of Quality factor of probe using DGS structures

Some of the most common DGSs that can be used to enhance the quality factor of 2D microstrip

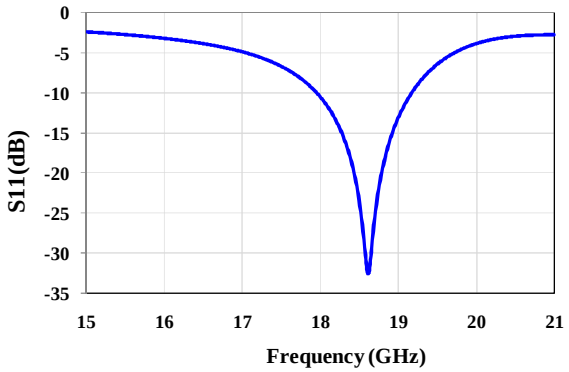

Fig. 2. Return loss of the primary probe

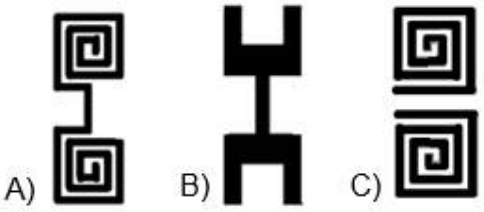

Fig. 3. Some of the different DGSs [22-24]

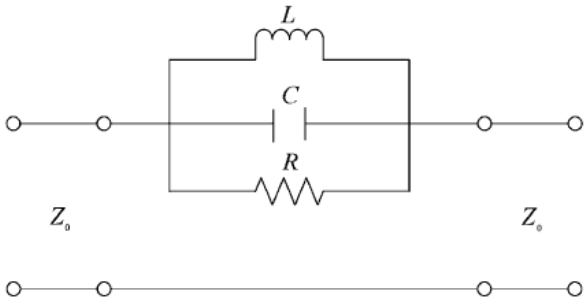

Fig. 4. Equevalent circuit ot U-shape DGS

filters, antennas and probes are shown in Fig. 3 [22-24].

All the slots in Fig. 3 are etched on the ground plane of the primary scheme of the probe and all these structures are simulated using HFSS software. In Fig. 5(a-c), the construction of probe with these DGSs is shown. Also, Fig. 5(d) demonstrates the reflection coefficients of the probe with these DGSs and the quality factor of probe with all DGSs are compared in Table II. Results show that the probe structure with two separate spiral DGS has a considerably greater quality factor. The structure of Fig. 3(c) designed by using U-shape slot on the ground plane has anequivalent circuit shown in Fig. 4. Also, C, L and R for this resonator are calculated through equations (4-6). Based on simulation results in Ansoft HFSS software, it is concluded that by increasing number of the rectangular slot the quality factor of the probe is improved significantly.

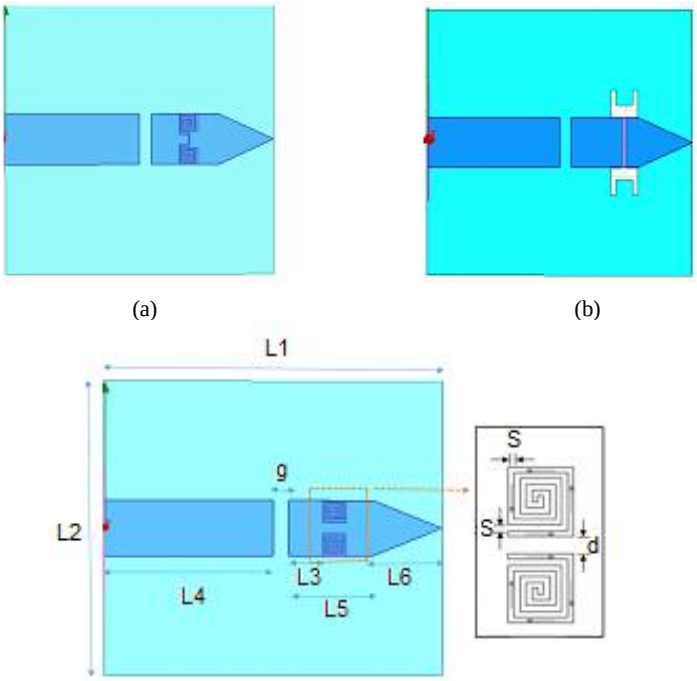

Fig. 5. (a),(b),(c) Probe construction with different DGSs, (d) Reflection coefficient of the probes

$$C = \frac{\omega_c}{2Z_o(\omega_o^2 - \omega_c^2)} \quad (4)$$

$$L = \frac{1}{4\pi^2 f_o^2 C} \quad (5)$$

$$R = \frac{2Z_o}{\sqrt{\frac{1}{S_{11}(\omega_o)^2} - \left(2Z_o\left(\omega_o C - \frac{1}{\omega_o L}\right)\right)^2} - 1} \quad (6)$$

Table II. Quality factor of the probes with different DGSs

Structure	Resonant frequency GHz	Quality factor
(a)	20.42	560
(b)	18.62	1026
(c)	18.62	8493

Table III. Final dimensions of the probe (in mm)

L1	L2	L3	L4	L5	L6	g	S	d
16	16	1.69	8	4	3.27	0.73	0.1	0.6

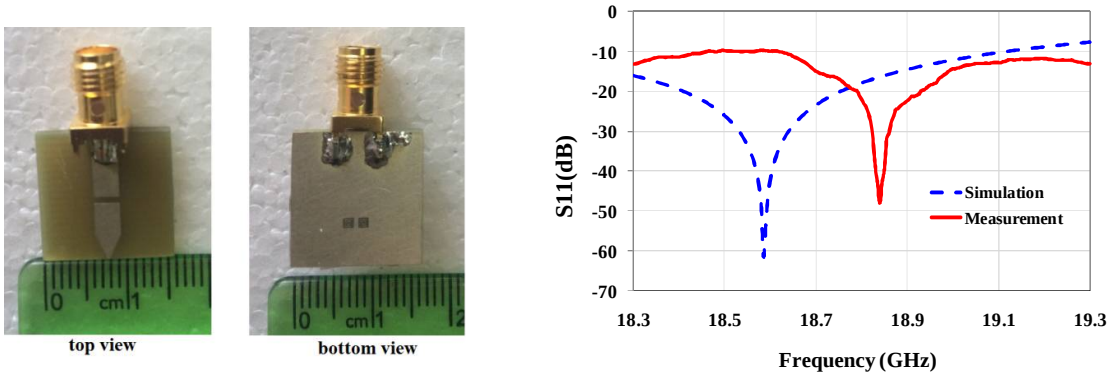

(a) (b)

Fig. 6. (a) Photograph of the manufactured probe, b) Reflection coefficient of the probe.

Therefore this structure (as shown in Fig. 5(c)) is selected for fabrication and experimentation. Tables III show the final computation of the probe dimensions with two separate spiral DGS for resonating at 18.5GHz.

Finally, the final designed probe is fabricated on a 1.6 mm thick FR4 substrate of dielectric constant 4.4. Simulation and measurements results for the probe reflection coefficient and photograph of the manufactured probe are shown in Fig. 6. Applied experimental set-up for our microwave measurements is discussed in the next section.

As shown in the Fig. 6, there is very good agreement between measurement and simulation of the probe's reflection coefficient. The error between simulated and measured response is 1.3% (200MHz) in frequency. This error is not a problem in our work because we want to use this probe for imaging of MUT. The changes in amplitude and resonance frequency of the probe in front of the MUT are very important.

III. EXPERIMENTAL RESULTS

In this section the resolution properties of the proposed probe for detection of invisible cracks with

different size are studied. The experimental set-up consists of a microwave resonator coupled to a feed line and connected to a network analyzer via a RF cable. The RF cable is also connected to a 0.0–20 GHz signal generator. The probe is mounted vertically over ax-y stage. During measurements, the stand-off distance between probe and sample is fixed and the sample was varied on the x-y stage by two stepper motors in x and y directions.

To modeling the cracks, as shown in Fig. 7(a-b), sheets of aluminum plates with different distances to be put together. Then for sub-surface imaging model, a paper sheet is placed on the crack. Distance between aluminum sheets varies from 10mm to 1mm. The operation frequency is fixed at 18.9GHz (the reflection resonance of aluminum plate) and standoff distance between probe and MUT is considered as 3mm. Probe scans a vector of 70mm length along the aluminum plates and cracks are placed exactly in the middle of scan vector. Two parameters including the amplitude and phase of reflection coefficient are monitored by the network analyzer and the results are recorded by Lab-View Software.

The simulation and measurement results in Fig.7 show that the magnitude of reflection coefficient is able to detect the edges of the invisible cracks with size of 2 mm and for a distance of 1 mm or less between aluminum plates, the probe cannot able to detect the crack and detection error rises. Phase of reflection coefficient in Figure 8 is well able to detect the edges of the cracks with a width of 10 to 2 mm. Also, results demonstrate that the average contrast for subsurface detection of crack is obtained about 20dB for amplitude and 300 degrees for phase of reflection coefficient.The error between measurement and simulation results are due to the noise of measurement and its condition compare to simulation which can be minimized by using image processing methods.

IV. CONCLUSION

High-Q near-field Microwave probe is designed and fabricated using defected ground structures for surface and subsurface crack detection in metal structures. For this purpose, several near-field probes with different DGSs are designed and probe with the highest quality factor is selected for subsurface detection. Then, a measurement scenario for detection of invisible cracks with different sizes is implemented. Experimental results show that the proposed probe is able accurately detect invisible crack of a size larger than 1mm with at least 20dB magnitude and more than 300 degrees phase contrast. It has also been demonstrated that the proposed device can efficiently used for detection and imaging of small failure and crack in dielectric and metallic structures.

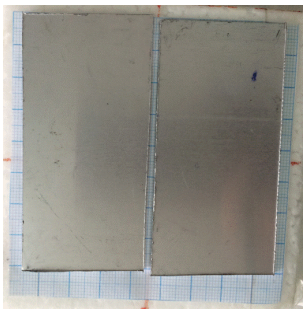

(a)

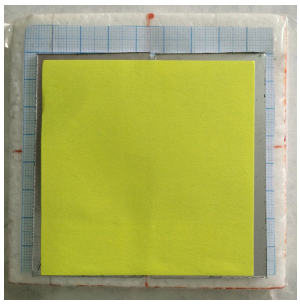

(b)

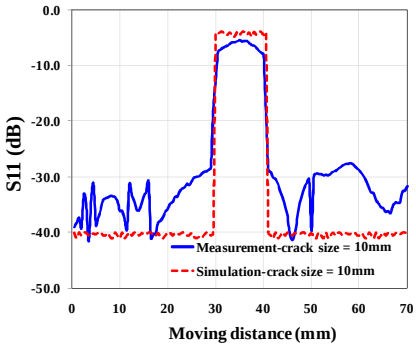

(c)

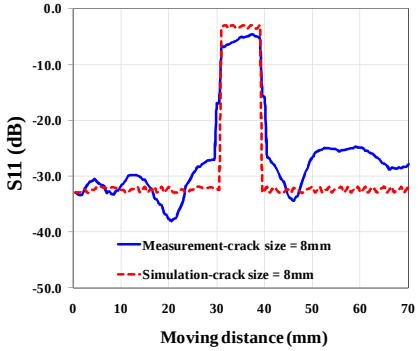

(d)

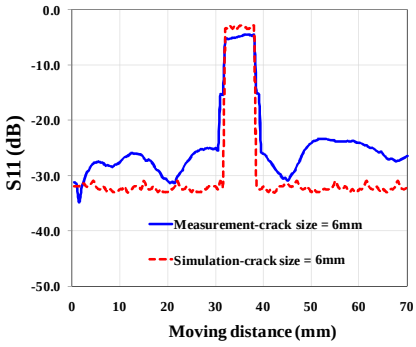

(e)

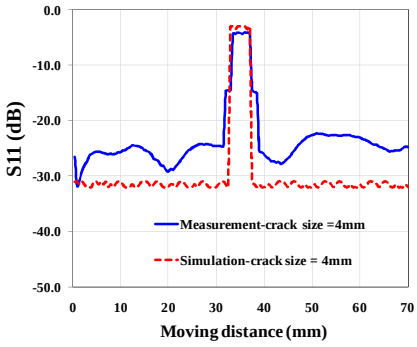

(f)

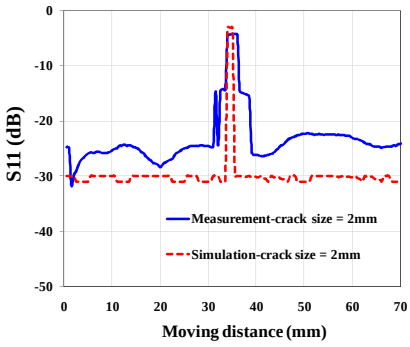

(g)

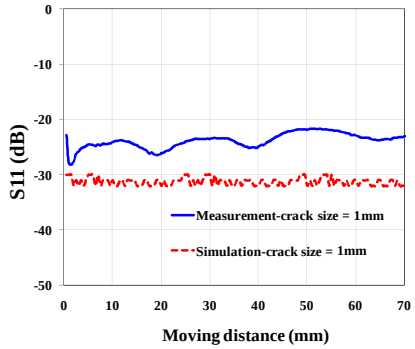

(h)

Fig. 7. Modeling the cracks, (a) sheets of aluminum plates with different distances without cover and (b) with cover. Magnitude of reflection coefficient for distance of (c) 10mm, (d) 8mm, (e) 6mm, (f) 4mm, (g) 2mm, (h) 1mm

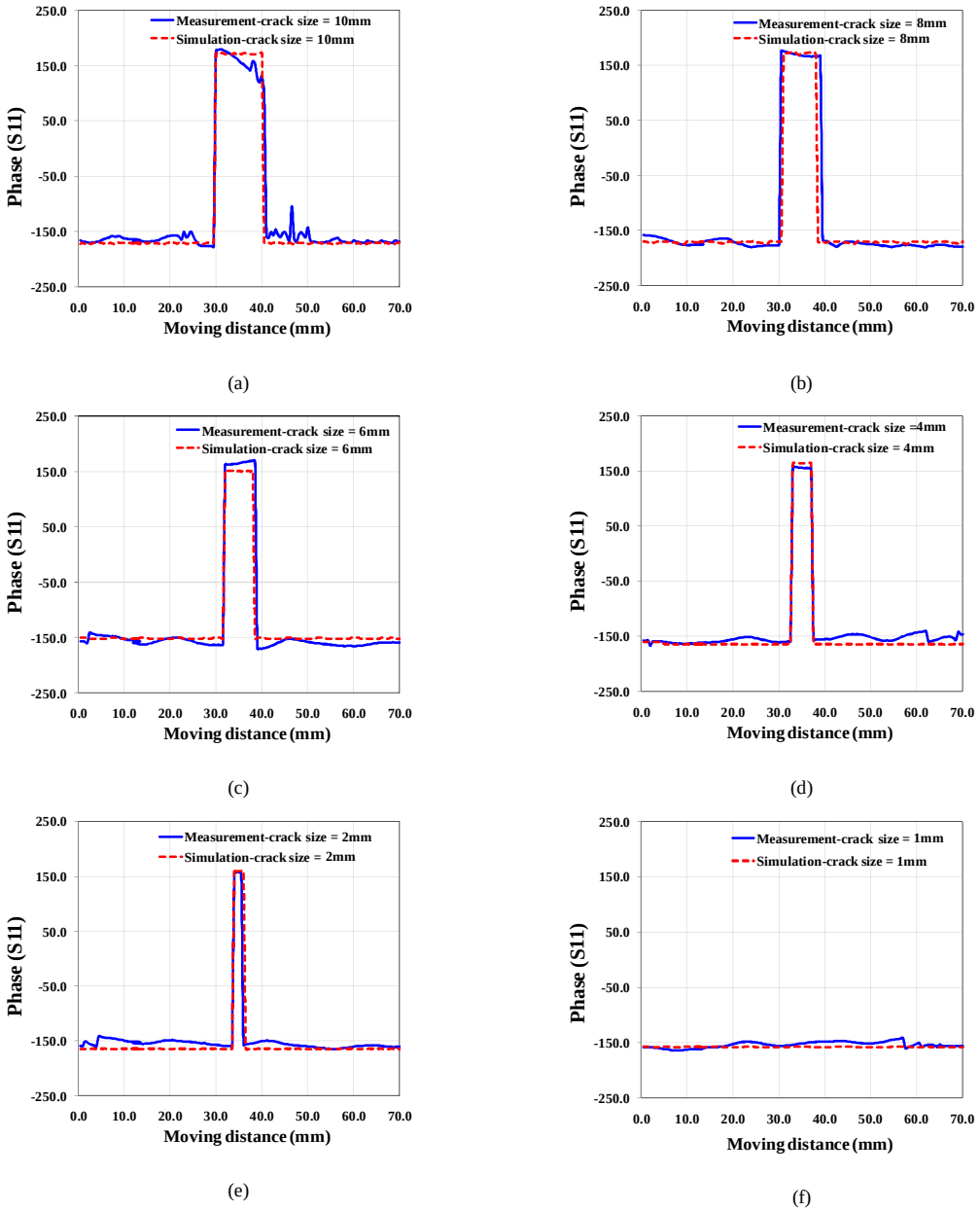

Fig. 8. Phase of reflection coefficient for distances of (a) 10mm, (b) 8mm, (c) 6mm, (d) 4mm, (e) 2mm, (f) 1mm

REFRENCE

[1] X. Zhuge and A.G. Yarovoy, "Three-Dimensional Near-Field MIMO Array Imaging Using Range Migration Techniques," *IEEE Trans. Image Processing*, vol. 21, no. 6, pp. 3026-3033, June 2012.

[2] L. Li, W. Zhang, and F. Li, "Derivation and Discussion of the SAR Migration Algorithm Within Inverse Scattering Problem: Theoretical Analysis," *IEEE Transactions on Geoscience and Remote sensing*, vol. 48 ,no. 1, pp. 415-422, Jan. 2010.

[3] M. Ghasr, M. Abou-Khousa, S. Kharkovsky, R. Zoughi, and D. Pom-merenke, "Portable real-time microwave camera at 24 GHz," *IEEE Trans. Antennas Propag.*, vol. 60, no. 2, pp. 1114–1125, Feb. 2012

[4] I. Lecomte, S.E. Hamran and L.J. Gelius, "Improving Kirchhoff migration with repeated local plane-wave imaging? A SAR-inspired signal-processing approach in prestack depth imaging", *Geophysical Prospecting*, vol. 53, no. 6, pp. 767-785, Nov. 2005.

[5] N. Nikolova, "Microwave imaging for breast cancer", *IEEE Microwave Magazine*, vol. 12, no. 7, pp. 78-94, Dec. 2011.

[6] E.C. Fear, J. Bourqui, C. Curtis, D. Mew, B. Docktor, and C. Romano, "Microwave Breast Imaging With a Monostatic Radar-Based System: A Study of Application to Patients," *IEEE Trans. Microwave Theory Techn.*, vol. 61 ,no. 5, pp. 2119-2128, May 2013.

[7] J.D. Shea, P. Kosmas, S.C. Hagness, and B.D. Van Veen, "Three-dimensional microwave imaging of realistic numerical breast phantoms via a multiple-frequency inverse scattering technique," *Med. Phys.*, vol. 37, no. 8, pp. 4210-4226, Aug. 2010.

[8] L.F. Chen, C.K. Ong, C.P. Neo, V.V Varadan, and V.K. Varadan "Microwave Electronics: Measurement and Materials Characterization,"*John Wiley & Sons Ltd.*, 2004.

[9] C. Gao, B. Hu, I. Takeuchi, and K.-S. Chang, "Quantitative scanning evanecsent microwave microscopy and its applications in the characterization of functional materials libraries," *Meas. Sci. Technol.* vol. 16, no. 1, pp. 248-260, Dec. 2004.

[10] M. Tabib-Azar and Y. Wang. "Design and fabrication of scanning near-field microwave probes compatible with atomic force microscopy to image embedded nanostructures," *IEEE Trans. Microwave Theory & Tech.*, vol. 52, no. 3, pp. 971-979, March 2004.

[11] C. Gao, T. Wei, F. Duewer, Y. Lu and X.-D. Xiang. "High spatial resolution quantitative microwave impedance microscopy by scanning near-field microscope,"*Appl. Phys. Lett.*,vol 71, no. 13, page 1872, 1997.

[12] B. Saleh, "Introduction to Sub-surface Imaging Handbook," Cambrige University Press, 2011.

[13] R. Zoughi and S. Kharkovsky, "Microwave and millimeter wave sensors for crack detection," Fatigue *& Fracture of Engineering Materials & Structures*, vol. 31, no. 8, pp. 695-713, Aug. 2008.

[14] P.J. Shull (Editor), "Nondestructive Evaluation: Theory, Techniques and Applications,"*Marcel Dekker*, New York, USA, 2002.

[15] R.J. Hruby and L. Feinstein, "A novel non-destructive non-contacting method for measuring the depth of thin slits and cracks in metals," *Rev. Sci. Instrum.* , vol. 41, no. 5, pp. 679-683, 1970.

[16] A. Husain and E.A. Ash "Microwave scanning microscopy for nondestructive testing," *Proc. 5th European Microwave Conf.*, Hamburg, Germany, pp. 213-217, 1975.

[17] A.J. Bahr, "Microwave eddy-current techniques for quantitative nondestructive evaluation. In: Eddy-Current Characterization of Materials and Structures (edited by G. Birnbaum and G. Free)," *American Society for Testing and Materials (ASTM)*, Philadelphia, PA, USA, STP 722, pp. 311-331, 1981.

[18] A.J. Bahr, Microwave Nondestructive Testing Methods, Gordon and Breach Science Publishers, 1982.

[19] R. Moradi,F. Kazemi, J. Ahmadi-shokouh, F. Mohanna, F. Jafari, "Design and fabrication of a near-field probe for sub-surface microwave imaging," *Telecommunications (IST), 2014 7th International Symposium on, IEEE*, 2014.

[20] D. M. Pozar, Microwave Engineering, 4th Edition, John Wiley , 2012.

[21] HFSS: High Frequency Structure Simulator Based on Finite Element Method 11, Ansoft Corporation.

[22] A. Boutejdar, S. Amari, A. Elsherbini, A. S. Omar, "A Novel Lowpass Filter with Ultra-Wide Stopband and Improved Q-Factor Performance Using H-Defected Ground Structure (DGS)," *Antennas and Propagation Society International Symposium*, IEEE, Honolulu, 2007.

[23] J. Choi C. Seo, "High-Q metamaterialinterdigital transmission line based on complementary spiral resonators for low phase noise voltage-controlled oscillator," *IET Circuits, Devices & Systems* , vol. 6, no. 3, p. 168-175, May 2012.

Duk-Jae Woo, Taek-Kyung Lee, Jae-Wook Lee, Cheol-Sig Pyo, Won-Kyu Choi., "Novel U-Slot and V-Slot DGSs for Bandstop Filter With Improved Q Factor," *IEEE Trans. Microwave Theory and Techniques*, vol. 54, no. 6, pp. 2840-2847, June 2006.